2
Literature Survey

2.1 REVIEW ON SIGNAL PROCESSING TECHNIQUES

Signal processing techniques enabled the designing of fast detection algorithms in distribution systems by extracting suitable transient features.

Fourier Transform (FT)

Fourier Transform (FT) is used for analyzing the time-varying continuous signal in the frequency domain. Here a signal is identified as a superposition of sinusoidal signals with different frequencies. This is of great help for the power system engineers to solve detection problems most efficiently. For any function $f(x)$, the Fourier Transform is denoted by $F(s)$ given by

$$F(s) = \int_{-\infty}^{\infty} f(x)e^{-j2\pi sx}dx \tag{2.1}$$

$$f(x) = \int_{-\infty}^{\infty} F(s)e^{j2\pi sx}ds \tag{2.2}$$

In both cases, $j = \sqrt{(-1)}$ and x is a time-varying signal in the time domain, and s corresponds to the frequency of the inverse time-domain signal.

However, FT cannot provide any transient information at a particular instant of time [Karimi *et al.*, 2000]. Time-frequency analysis was made possible by using Short-time FT (STFT). It overcomes the drawback of FT by considering short windows or frames. The analysis is performed within the window. By sliding the window over the signal, the signal's time-frequency analysis is achieved [Dash *et al.*, 2003]. However, its application is limited to stationary signals due to the disadvantage of fixed window size, and a compromise needs to be made with the frequency resolution [Zhao *et al.*, 2004]. For identifying transients in disturbance signals, a small window can be selected [Gu and Bollen, 2000]. Discrete FT (DFT) extends the application of FT to discrete-time signals obtained by sampling continuous-time signals with a sampling frequency. The DFT algorithm did not gain prominence until the development of the Fast Fourier Transform (FFT) by Cooley and Tukey in 1965 [Cooley and Tukey, 1965]. The frequency-domain analysis of discrete-time signals was made computationally efficient by the computation of DFT using the FFT algorithm Ribeiro *et al.* [2013]. One of the limitations of the FFT is its misrepresentation of the high-frequency components as low-frequency ones [Lee and Girgis, 1988]. Goertzel algorithm (GA) falls under the class of DFT with its fast capability for pitch detection compared to DFT and FFT [Kim *et al.*, 2011].

Wavelet Transform (WT)

Wavelet Transform (WT) is one of the premier techniques for the time-frequency analysis of a signal. Small waves characterize the signal called wavelets. These wavelets are generated from a function called the mother wavelet. By dilating and contracting the wavelets, the WT can also be applied to nonstationary signals. The dynamic behavior, discontinuities, and transient nature can

be localized efficiently as the wavelets have large windows at low frequencies and short windows for high frequencies [Graps, 1995].

Wavelet transform (WT) is similar to the Fourier transform (FT) with a different merit function. The main difference is that FT decomposes the signal into sine and cosine functions, i.e., the function is localized in the Fourier space, whereas WT uses functions that are localized in both the real and Fourier space, which can be expressed as,

$$WT(\alpha,\tau) = \int_{-\infty}^{\infty} h^*_{\alpha,\tau}(t) f(t) dt \tag{2.3}$$

$$h^*_{\alpha,\tau}(t) = \alpha^{-1/2} h\left(\frac{t-\tau}{\alpha}\right) \tag{2.4}$$

The wavelet function $h^*_{\alpha,\tau}$(t) and the signal $f(t)$ is the inner product of the complex conjugate, and it is represented as WT(α,τ). The Wavelet function $h^*_{\alpha,\tau}$(t) is proportional to the reciprocal of the frequency, where the variables α, τ and h are represented as scale parameter, translation parameter, and mother wavelet respectively. It is classified as continuous (CWT) or discrete (DWT). However, its performance suffers in the presence of noise and improper selection of the mother wavelet.

S-Transform (ST)

S-Transform (ST) addresses the shortcomings of the WT by consolidating the properties of WT and STFT. It employs a moving Gaussian window and is also scalable to obtain time-frequency information [Stockwell *et al.*, 1996]. Localization of imaginary and real spectra are obtained simultaneously using ST. In ST, the idea of CWT is extended in which a modified wavelet transform is used as a time-frequency spectral localization technique. The $CWT(\tau, d_i)$ is a scaled replica of the fundamental mother wavelet, and it is defined as:

$$CWT(\tau, d_i) = \int_{-\infty}^{\infty} f(t)\omega(t-\tau, d_i) dt \tag{2.5}$$

The dilation d_i determines the width of the wavelet $\omega(\tau, d_i)$ which is used for resolution control. The critical feature of ST is the frequency-dependent resolution of the time-frequency space without any change or loss of local phase information. The ST is expressed as:

$$ST(t,f) = \int_{-\infty}^{\infty} h(t)\left(\frac{|f|}{\sqrt{2\pi}}\right) e^{\left(\frac{-(\tau-t)^2 f^2}{2}\right)} e^{-j2\pi f t} dt \tag{2.6}$$

$$g(t) = \left(\frac{1}{\sigma\sqrt{2\pi}}\right) e^{\left(\frac{-t^2}{2\sigma^2}\right)} \tag{2.7}$$

$$\sigma(f) = \left(\frac{1}{|f|}\right) \tag{2.8}$$

where, $f(t)$, $g(t)$, and $\sigma(f)$ are the signal, scalable window, and control parameters of the Gaussian window, respectively. ST offers superior frequency resolution for lower frequencies and better time-frequency resolution for higher frequencies. It offers multi-resolution of the signal without affecting the phase of respective frequency components and hence finds its application in disturbance detection in the presence of noise[Ventosa *et al.*, 2008].

TT transform (TT-T)

TT transform (TT-T) is based on ST, which represents one-dimensional (1D) time-series data as a two-dimensional (2D) time-time series. With the help of scaled windows, the TT-transform provides a better localization of the signal than ST [Pinnegar and Mansinha, 2003].

Gabor-Wigner Transform (GWT)

Dennis Gabor proposed a special case of STFT, formulates into the Gabor transform (GT). This transform is beneficial as the phase content of the local divisions and sinusoidal frequency of a signal. It can also be determined with its change over time. GT signal $S(\tau, \omega)$ is expressed as:

$$S(\tau, \omega) = \int_{-\infty}^{\infty} f(t)g(t-\tau)e^{-j\omega t}dt \tag{2.9}$$

where, the amount of the time shift is represented by τ and window function represented by $g(t)$. The center μ_t and radius Δ_t are individually calculated as follows:

$$\mu_t = \frac{\int_{-\infty}^{\infty} t \times |g(t)|^2 dt}{\int_{-\infty}^{\infty} |g(t)|^2 dt} \tag{2.10}$$

$$\Delta_t = \sqrt{\frac{\int_{-\infty}^{\infty} (t-\mu_t)^2 \times |g(t)|^2 dt}{\int_{-\infty}^{\infty} |g(t)|^2 dt}} \tag{2.11}$$

The width of the window function is equal to $2\Delta_t$ and the interval range spans from $\mu_t - \Delta_t$ to $\mu_t + \Delta_t$. The cross-terms problem of Wigner distribution function and the limited resolution by Gaussian like window of Gabor transform are resolved by combining the merits of both to obtain better time-frequency information. Gabor–Wigner transform [Cheng *et al.*, 2015] is employed in extracting the frequency information with respect to time.

Kalman Filter (KF)

R.E. Kalman introduced a recursive solution to the discrete data linear filtering problem in 1960 [Kalman, 1960]. GF Welch and G Bishop gave the modern definition of Kalman Filter (KF) [Welch *et al.*, 1995]. It is a set of scientific equations that affords a practical computational means to determine the state of a process, in a design that reduces the mean of the squared error. In this filter, the information in the past states is stored and used for calculating the subsequent states. The current estimation is calculated based on the preceding state information using the following equation.

$$\hat{x}_k = K_k Z_k + (1 - K_k)\hat{x}_{(k-1)} \tag{2.12}$$

where, $\hat{x}_k$= current state estimate, k = discrete time intervals, $k = 1$ can be taken as 1 ms & $k = 2$ as 2 ms, Z_k = measurement value, K_k = Kalman gain which varies between 0 and 1, $\hat{x}_{(k-1)}$ = previous state signal. Kalman gain (K_k) is the unknown component of the given equation. This gain is calculated based on the measured values, and the preceding estimated signal. Kalman filtering theory is an efficient technique to extract harmonic signatures from the fault currents [Samantaray *et al.*, 2009a].

Mathematical Morphology (MM)

The mathematical morphology (MM) technique was originally developed by George Matheson [Kingman, 1975] and Jean Serra [Serra, 1982] for signal analysis in the time domain itself with the help of morphology filters. It depends on concepts of set theory and integral geometry, which analyzes the signal's shape and has its application in the image processing field. The basic idea is to use a structural element as a probing tool to collect the information from the signal. It

involves dilation or expanding process and erosion or shrinking process as operators for decomposing a signal into various structures that give meaningful information [Maragos and Schafer, 1987].

In this technique dilation and erosion have been considered as fundamental operators and operation is based on the addition or subtraction of $f(n)$ and $g(n)$ in an $M-$length mobile window. These operators are further utilized to extract the desired features.

$$dilation: \ (f \oplus g)(n) = max\{f(n-m) + g(m)\} \tag{2.13}$$

$$erosion \ (f \ominus g)(n) = min\{f(n+m) - g(m)\} \tag{2.14}$$

where, the range for dilation is $m = \{0, 1, \cdots, M-1\}$; $n = \{M-1, M, \cdots, N-1\}$ and the range for erosion is $m = \{0, 1, \cdots, M-1\}$; $n = \{0, 1, \cdots, N-M\}$, with one dimensional signal is represented by $f(n)$ in the domain: $D[f] \subset E$ and the structure element is denoted by $g(n)$ in the domain: $D[g] \subset E$. Any two combination of fundamental operations can generate many operations,

$$Open \ operator (f \circ g) = (f \ominus g) \oplus g \tag{2.15}$$

$$Close \ operator (f \bullet g) = (f \oplus g) \ominus g \tag{2.16}$$

$$Open - close \ operator \ OC(f) = f \circ g \bullet g \tag{2.17}$$

$$Close - open \ operator \ CO(f) = f \bullet g \circ g \tag{2.18}$$

The open circle is represented by $\circ$ (opening), and a close circle is represented by $\bullet$ (closing). The opening of f by g is obtained by the erosion of f by g, followed by dilation of the resulting by g. Similarly, the closing of f by g is obtained by the dilation of f by g, followed by the erosion of the resulting structure by g. After calculating the fundamental operators by MM, power system disturbance detection is achieved by extracting desired features from signals. Morphological gradient wavelet, MM, and digital filtering with some basic terminology and mathematical description have been discussed by [Chen *et al.*, 2009]. MM-based features are utilized to detect high impedance faults in [Gautam and Brahma, 2013].

Hilbert-Huang Transform (HHT)

HHT is reported to be one of the best techniques for processing non-linear and nonstationary signals. Two steps are involved in this technique. Firstly, the signal is decomposed into independent components called intrinsic mode functions (IMFs), leaving behind a monotonic residue using EMD. Secondly, the Hilbert spectrum is obtained by applying Hilbert Transform on decomposed components or IMFs [Huang *et al.*, 1998]. HHT can be applied to nonstationary signals, unlike FT, which is restricted only to stationary signals [Donnelly, 2006]. Several limitations of WT like decomposition dependence on the mother wavelet selection, leakage energy, and distortion at borders leading to spikes are overcome by adaptive decomposition of HHT. It also provides better resolution in the time, and frequency domain than ST as the latter is unsuitable for all practical signals [Peng *et al.*, 2005]. The detailed mathematical analysis is discussed in Chapters 3 and 4. IMFs being oscillatory in nature are utilized in the literature for various fault diagnosis applications. IMFs based on kurtosis are utilized in finding faults in internal combustion engines in [Nidadavolu *et al.*, 2009]. Power quality events are detected using the first three IMFs which contain high-frequency content in [Shukla *et al.*, 2009]. A bus bar protection scheme is proposed in [Guo *et al.*, 2015], utilizing the first intrinsic mode function. Balanced and unbalanced faults in the Self Excited Induction Generator (SEIG) system are detected using the IMF's obtained from negative sequence components of current signals in [Dalei and Mohanty, 2016]. IMF's are selected using Mutual Information (MI) for protection of 14 bus microgrid in [Gururani *et al.*, 2016]. Islanding event detection [Chaitanya and Yadav, 2018] and transmission line fault detection [Anand and Affijulla, 2020] are also achieved based on features from IMFs.

Table 2.1: Comparison of various SP techniques.

SP Technique	Advantages	Disadvantages
DFT	Efficient and fast to obtain frequency information from stationary signals	Cannot provide the time-frequency information simultaneously.
STFT	Easy to implement and gives time-frequency information of non stationary signals.	Fixed window does not make it suitable for multi-resolution applications.
WT	Provides time of occurrence of a particular frequency band or harmonic information.	Requires a suitable mother wavelet and is not suitable for noisy signals.
ST	It provides phase and frequency information and has better anti-noise performance.	The Gaussian window is not adaptive and it requires a high computational burden.
KF	It provides an efficient estimation of the harmonic components of fault currents.	It requires great amounts of computation and additional efforts for accuracy of parameters.
GWT	Suitable for non-stationary signal analysis as it compensates for the low clarity and the cross-term problem of Gabor Transform and Wigner Distribution function.	The analysis is the most complicated, calculation-wise.
EMD	It is an adaptive and data driven technique and it does not require predefined set of mathematical or basis functions.	Mode mixing may lead to loss of data during denoising.
HHT	It provides instantaneous features corresponding to changes in amplitude and phase. It is robust to noise and very adaptive.	Its performance deteriorates and becomes complex for wide band signals.

However, residue based statistical features which have a potential to avoid a separate selection method of IMFs for fast detection and classification of faults in distribution system are not reported and hence proposed in this thesis work [Shaik *et al.*, 2019b]. Instantaneous features from the first-level residue resulted in faster detection of faults in the presence of RES as proposed in this work Shaik *et al.* [2019c]. As each and every signal processing technique have their pros and cons the widely used SP techniques are enumerated in the Table 2.1, for proper selection.

2.2 TYPES OF PROTECTION ALGORITHMS

Since the power system events are associated with transients, signal processing (SP) techniques are vital in extracting the features associated with disturbances. There are two types of protection algorithms designed to address these issues: threshold-based techniques and machine learning (ML)-based techniques. The various steps in the threshold-based techniques are shown in Fig. 2.1, which firstly involves data acquisition where the current or voltage signal is measured, and the sampling frequency and the moving window length are decided. It is followed by processing the signal using a suitable signal processing technique. The choice of the SP technique is dependent on the time or frequency-based information required for the task. In the next stage, features are extracted based on the statistical properties like mean, skewness, kurtosis, standard deviation, etc., for the various events involved. In the feature selection stage, only distinct features are selected by eliminating redundant information. This step sometimes involves a feature optimization algorithm where the feature set extracted is extensive. After selecting suitable features, a fault index is computed using the post-disturbance data. It is ensured that the post-disturbance data is chosen as minimum as possible for faster diagnosis. The last stage is a decision-making step in which the fault index is compared with predefined thresholds for classifying any number of classes like islanding and power system faults. These thresholds are set after the complete study of the system is considered. Hence, any variation in the system, like variation of RES capacity, may lead to false tripping. ML-based adaptive techniques are more suitable and prove to be more efficient in the presence of noise and other system variations. The difference in this method can be observed after the feature selection stage. The selected features are fed as input to train a machine learning model and later tested with the untrained dataset to detect or classify events, as shown in Fig. 2.2. The fault index computation and manual thresholds can be avoided in this method.

2.3 THRESHOLD BASED ALGORITHMS FOR ISLANDING AND FAULT DETECTION

This section reviews the threshold-based techniques from the literature, focusing on islanding and fault detection times with signal processing methods.

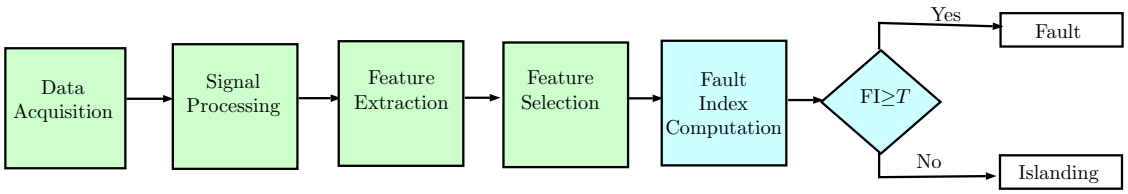

Figure 2.1: Threshold based algorithm.

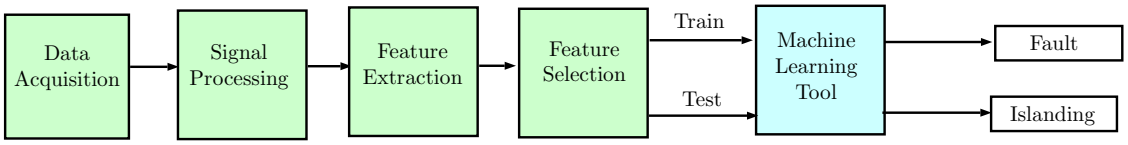

Figure 2.2: Machine learning based algorithm.

A. International islanding standards

Many international islanding standards are formulated, which serve as guidelines to safely operate the grid involving grid forming or grid following modes of DG. The control operation of the converter differentiates the modes of operation. A grid following mode involves the control of the current injected by the converter with a particular phase difference to the grid voltage at the PCC. Therefore, obtaining the grid voltage's fundamental frequency phasor is necessary. The outer loops modify the amplitude and phase of the converter reference current according to the grid voltage such that the required active and reactive power can be injected. A grid-forming mode controls the voltage magnitude and phase angle at PCC. Thus it is not always essential to obtain the grid voltage's fundamental frequency phasor at PCC. Additional outer loops may be required depending on the network characteristics to which the converter is connected to adapt the injected instantaneous active and reactive power and provide frequency and voltage support [Zuo *et al.*, 2021].

A few of the widely used islanding detection standards are UL1741 (Underwriters Laboratories Inc.), IEEE 1547 [Photovoltaics and Storage, 2018], IEC 62116 (International Electrotechnical Commission), IEEE 929 [Wu *et al.*, 2017], VDE 0126-1-1 (German Standard), AS4777.3-2005 (Australian Standard), Korean Standard and Japanese Standard [Ahmad *et al.*, 2013]. The detection time requirements for islanding, voltage, and frequency limits according to various international standards are compared in Table 2.2, where, V_n and f_n represent nominal voltage and frequency, respectively.

B. Classification of Islanding detection Methods

Islanding detection is achieved by the measurements at the utility side, also known as remote detection, or at the DG side, called local detection. Remote techniques are highly reliable, have no impact on PQ, and have no Non Detection Zone (NDZ) but require communication infrastructure, high implementation cost, and complex design. NDZ is the term related to the mismatch in the active and reactive powers where the discrimination of islanding events with non-islanding events becomes critical [Lopes and Sun, 2006]. The most widely used techniques are power line carrier communication (PLCC) method [Xu *et al.*, 2007], transfer trip scheme [Bayrak, 2015] and PMU based scheme [Kumar and Bhowmik, 2018].

Table 2.2: International islanding Standards.

Standards	Islanding Detection Time	Acceptable Voltage Range	Acceptable Frequency Range
UL1741, IEEE 1547, IEEE 929	IDT $<$ 2 s	59.3 Hz $\leq f_n \leq$ 60.5 Hz	88% of $V_n \leq V_n \leq$ 110% of V_n
IEC 62116	IDT $<$ 2 s	$f_n - 1.5Hz < f_n; f \leq f_n + 1.5Hz$	88% of $V_n \leq V_n \leq$ 110% of V_n
VDE 0126-1-1	IDT $<$ 0.2 s	47.5 Hz $\leq f_n \leq$ 50.2 Hz	80% of $V_n \leq V_n \leq$ 115% of V_n
Korean Standard	IDT $<$ 0.5 s	59.3 Hz $\leq f_n \leq$ 60.5 Hz	88% of $V_n \leq V_n \leq$ 110% of V_n
AS4777.3-2005	IDT $<$ 2 s	Setting Value	Setting Value
Japanese Standard	IDT $<$ 0.5 s	Setting Value	Setting Value

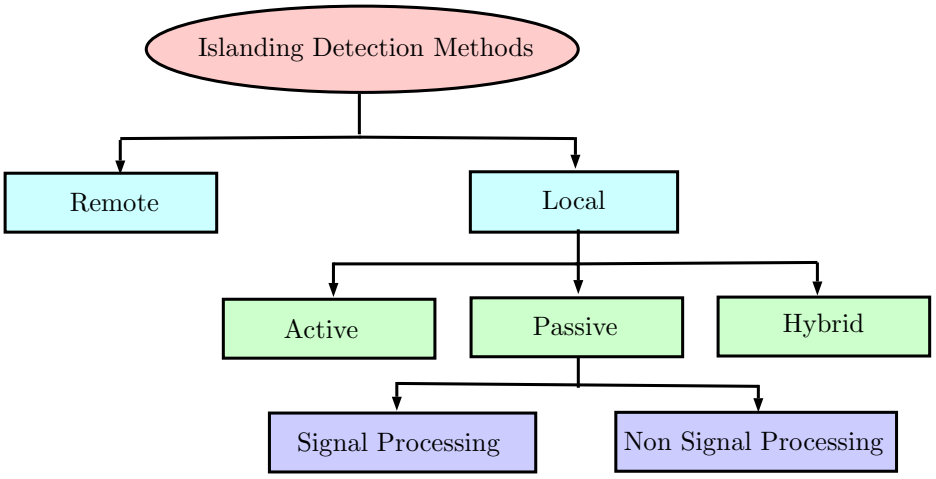

Figure 2.3: Islanding detection methods.

Local islanding detection methods (IDMs) are categorized as active, passive (nonsignal processing), Passive (signal processing techniques), and hybrid methods. The IDMs are classified as shown in Fig. 2.3. Active methods involve actively perturbing voltage or frequency or both in the grid. Islanding is detected if any change in the grid is observed. They require additional power electronic devices/controller, requires complex design and causes PQ issues. The various active techniques proposed in the literature are impedance measurement [Chiang *et al.*, 2010], harmonic injection [Hamzeh *et al.*, 2016] , slip mode frequency shift (SMS) [Mohammadpour *et al.*, 2017], active frequency drift (AFD)[Wen *et al.*, 2015], Sandia frequency shift (SFS) [Hatata *et al.*, 2018], Sandia voltage shift (SVS) [Vazquez *et al.*, 2020], Frequency jump (FJ) [Bartoccini *et al.*, 2009], Active power and reactive power injection [Hou and Chen, 2013], virtual capacitor and inductor scheme, [Chiang *et al.*, 2012] and, General electric frequency schemes (GEFS) [Mishra *et al.*, 2019].

Passive methods detect islanding by passive measurements of various parameters or monitoring the system's state. They are classified as non-signal processing based and signal processing-based passive methods. These methods have faster detection times, are cost-effective, and do not cause PQ issues. The non signal processing techniques measure various parameters like Over/Under voltage, and frequency [Reddy and Sreeraj, 2019], Phase jump detection (PJD) [Pourbabak and Kazemi, 2014], Voltage harmonics distortion [Jang and Kim, 2004], Rate of Change of Power (ROCOP) [Laghari *et al.*, 2015], Rate of Change of Frequency (ROCOF) [Gupta *et al.*, 2014], Rate of Change of Frequency over Power (ROCOFOP) [Rabuzin *et al.*, 2021], Change of Impedance [Xie *et al.*, 2020] and Voltage Unbalance [Makwana and Bhalja, 2017].

Hybrid methods combine active and passive methods for better results and backup. These include voltage and reactive power shift Shi *et al.* [2020], SFS and Q-f based scheme [Sirjani and Okwose, 2016], positive feedback and voltage unbalance [Nayak *et al.*, 2020] and SFS and ROCOF [Khodaparastan *et al.*, 2015].

C. Signal Processing Based Passive Techniques

Here the main focus is on signal processing and machine learning techniques; therefore, the other methods are only briefly mentioned above. The active methods are employed with caution though they do not have significant NDZ issues as they cause power quality issues. Though non-signal processing passive methods have a fast response time, they have undesirable large NDZ. SP-based methods are handy for minimizing NDZ since they can extract latent features from the measured signal and reveal much information about the system's state. An islanding event can be detected based on the event-specific information from the extracted features. The application of SP methods for islanding detection by feature extraction are further explained.

(a) FT

In [Kim, 2012], a DFT-based IDM is proposed in which the harmonics from the grid voltage are used as features to detect islanding in 1ms in the presence of a photovoltaic (PV) renewable energy source. DFT-based GA algorithm is utilized to find the harmonic content in the voltage at PCC [Kim *et al.*, 2011]. The detection time reported is under two cycles.

(b) WT

In [Zhu *et al.*, 2008], CWT and Mallat decomposition is applied to the voltage signal at the DG. First wavelet denoising of the signal is done, and later Mallat decomposition is employed to obtain features from first and second-level detail coefficients. As CWT involves more computation due to the generation of many coefficients, DWT-based methods are investigated.

In [Hsieh *et al.*, 2008], an IDM is proposed using decomposition of voltage and frequency signals using Daubechies mother wavelet up to three levels. The islanding is detected when the variation in the measured quantities is above a threshold of 0.1. It is reported that the algorithm using Daubechies efficiently implements a field-programmable gate array (FPGA). This algorithm is also immune to other events like notch disturbance and voltage sag.

A hybrid method is presented in [Pigazo *et al.*, 2008] where the PCC voltage and current signals are monitored along with the injection of high-frequency components by the inverter interfaced DG system. One hundred thirteen wavelets from the families of Daubechies, Symlets, Coiflets, Biorthogonal, and Reverse Biorthogonal families have been tested and found that bi-orthogonal 1.5 mother wavelet provided better response time and time-frequency resolution. This method required fewer sensors and less computational burden.

In [Samantaray *et al.*, 2009b], negative sequence components of current and voltage signals are utilized at the DG terminals. These signals are decomposed using the db4 mother wavelet, and level-1 coefficients are obtained. The standard deviation and the change in the energy are used as features to compare with a threshold to detect the islanding event in one cycle. The algorithm is tested on a 10 MVA,25 kV system with four wind farms of 1.5 MW capacity each. The algorithm is not affected by the opening of breakers, load variations, and DG tripping in a noise-free environment. On the same test system, faults are also simulated, and separate thresholds for faults and islanding are proposed to detect within half cycle using wavelet alienation coefficients of current signals [Kolavennu and Shaik, 2019].

The authors in [Hanif *et al.*, 2010] reported that the db4 wavelet has compactness and localization properties to minimize the NDZ. A dyadic wavelet transform which is nothing but a DWT with Mallat's pyramid algorithm is used to decompose three-phase voltage signals at PCC to obtain second-level coefficients. The energy per two cycles is used as a feature to detect islanding in a 50 Hz grid-connected PV system of 4.2 kW. This work is extended experimentally in [Hanif *et al.*, 2012].

The voltage signals are decomposed using a db5 wavelet up to five levels for a grid-connected wind turbine system [Karegar and Sobhani, 2012]. If the coefficients of d5 are greater than a threshold of 3, then islanding is detected. It is proven that the algorithm is not affected by load variations, starting the induction motor, or capacitor bank switching. The islanding is detected in 0.2s on a 50 Hz system. A similar approach is followed on a grid-based inverter system of 2.5 kW. The voltage signals are decomposed, and first-level detail coefficients are used [Sharma and Singh, 2012].

A DWT-based algorithm with Haar wavelet is proposed in a 12 bus system with two synchronous DGs. The current signals at the DG terminals are decomposed to three levels, and features are compared with a threshold to detect the islanding. Haar wavelet ensured the detection in less than is 5.5 ms on a 60 Hz system. It is not affected by switching transients of the capacitor bank, induction motor starting, or opening of line breaker [Shariatinasab and Akbari, 2010].

The overlap of high frequencies results in information loss while applying DWT. This problem is addressed by applying wavelet packet transform (WPT) [Morsi *et al.*, 2010]. A new index named node rate of change of power is proposed. The three-phase current and voltage signals are measured to compute the power signal. This signal is decomposed using db10 mother wavelet up to four levels. This algorithm detects the islanding in 0.06 s when tested on a three bus system integrated with the 9 MW wind farm. The algorithm is not affected by voltage sags, faults, or sudden load change.

An IDM combining the benefits of the wavelet transform, Shannon entropy, and singular value decomposition (SVD) is proposed in [Samui and Samantaray, 2012] to obtain a Wavelet singular entropy index (WSEI). The three-phase voltage signals are decomposed with db4 wavelet up to four levels. The detection was achieved in a half cycle. However, faults or noise cases are not considered.

(c) ST

ST-based IDM is proposed on a grid-connected hybrid DG system in [Ray *et al.*, 2010]. Photovoltaic, wind energy, and fuel cells are connected. The negative sequence voltage signal is obtained from the three-phase voltage signals at PCC through a sequence analyzer and processed to obtain S-matrix. The energy and Standard deviation of the S-Contour are used as features to propose a threshold for islanding. The authors extended the work to make the algorithm immune to nonlinear load rejection and notch in a noisy environment of 20 dB SNR [Ray *et al.*, 2011]. It is reported that the negative sequence voltage signal is immune to noise, and ST performs well, but WT fails at 20 dB SNR noise. The algorithm is further extended to detect islanding in the presence of PQ disturbances, fault, and sudden load switching at 20 dB SNR [Ray *et al.*, 2012]. The islanding is detected in 26ms for ST and 28ms for WT.

The authors in [Samantaray *et al.*, 2010] utilized the negative sequence current and voltage signals at DG terminals to obtain the S-matrix. Spectral energy is calculated, and a new index Cumulative sum of spectral energy (CUSUM) is proposed for islanding detection in the presence of a wind farm of 9 MW. It is shown that change in the measurement at DG locations affects detection accuracy. It is reported that islanding is detected with 100% accuracy when the DG is closer to PCC and 92.3% accuracy when it is far away. Switching of load and capacitor and DG trip cases

are considered without fault or noise.

Though the performance of ST is better than WT in the presence of noise, it suffers in localizing transient disturbances effectively. A modified S-transform known as hyperbolic ST (HST) is proposed for detecting PQ events in which a pseudo-Gaussian hyperbolic window function is used [Biswal *et al.*, 2009]. Due to its asymmetrical nature, this provides better time and frequency resolutions at lower and higher frequencies. The window function has frequency dependence on its shape in addition to its width and height [Huang *et al.*, 2010]. In [Mohanty *et al.*, 2012], the negative sequence voltage signal is processed with HST to obtain the energy and standard deviation of the HST contour. These features are used to propose a threshold of 0.4 p.u and 7.5 p.u for energy and STD, respectively. When processed with the S-transform, the negative sequence components have shown better results in the presence of noise when compared to WT.

(d) TT-T

TT-T is utilized for obtaining the 2D TT contours for three-phase fault, islanding, and normal conditions [Khamis *et al.*, 2012]. The one-dimensional voltage signal at the DG location is processed to obtain the 2D TT contours. It is observed that the contours differentiate the islanding event from the other events considered. However, the performance is not evaluated in the presence of noise. The authors in [Mohanty *et al.*, 2012], in their work on grid integrated hybrid DG system, have proved that the TT-T performs better than the WT and ST in the presence of noise. Energy and standard deviation features are proposed to compare with a threshold for islanding detection. The algorithm is very efficient in differentiating the PQ transients in the presence of 20 dB SNR noise.

(e) MM

In [Mohanty *et al.*, 2014], MM is applied for islanding detection in an IEEE 30 bus system integrated with hybrid DG of PV and wind energy. Variations in dilation and erosion operations on voltage signals at PCC are applied to find the structural differences in the signal. Three differences in the generalized opening and closing, open and close, and erosion and dilation are considered. It is established that MM requires less computation when compared to the frequency domain analysis of the signal. This algorithm is immune to PQ in the presence of noise.

The voltage and current signals acquired at the DG location are processed with an MM filter proposed as dilate erode difference filter (DEDF) in [Farhan and Swarup, 2016]. The output is then processed by another operator named the average difference between maximum and minimum values of DEDF. Finally, an islanding index is proposed as a ratio index (MMRI). If it exceeds the threshold of 1.23, the islanding is detected. The algorithm is tested on a three-distribution line system with two wind and one synchronous diesel generator along with switching transients, faults, motor starting, feeder, and transformer switching.

(f) EMD and HHT

In [Niaki and Afsharnia, 2014], an IDM using EMD of the voltage signal at PCC over a moving window of one cycle is reported. The first IMF obtained after EMD is utilized for fixing a threshold value of 0.01 p.u. The algorithm is tested on a grid-connected inverter-based single and multiple DGs in the presence of a noisy environment of 20 dB SNR. It is confirmed that EMD is simple and requires less computation when compared to other techniques. The islanding is detected in less than two cycles showing immunity to DG tripping. However, faults are not considered. Both voltage and current signals with a sampling frequency of 1.2 kHz are measured at PCC in [Chaitanya and Yadav, 2018]. The ratio of the first IMFs of current and voltage is used as an index. This index

is compared with a threshold of 1.1 to detect islanding in 17ms.

An application of EMD to the reactive power signal at PCC of a radial three-node system connected with inverter-based DG is presented in [Thomas *et al.*, 2020]. The maximum energy of the first level IMF is considered a potential feature for detecting islanding by comparing it with a threshold. HHT is also applied to obtain the instantaneous energy of the signal as a second feature to increase the algorithm's reliability. The faults, islanding, and switching transients can be differentiated with the help of thresholds and the k-means clustering technique. This algorithm is later validated on an IEEE 14 bus system to detect the events within two cycles or 40 ms. However, the performance is not evaluated in the presence of noise.

The authors in [Khosravi *et al.*, 2021] proposed an algorithm in which the voltage signal is measured at the PCC to obtain the positive sequence of the voltage signal variation. EMD is applied to this signal to obtain the first level IMF, whose energy is used as a feature vector. Islanding is detected if the signal energy is above the threshold for six consecutive cycles for the distribution system considered or 3.5 cycles for an IEEE 34 bus system. This proposed algorithm is not affected by faults and switching transients due to linear and non-linear loads, motor, or capacitor. However, there is no threshold to differentiate faults from switching transients, and the effect of noise is also not considered.

(g) Integrated Techniques

Combined features of HHT and S-transform are also researched for faster fault detection, and classification [Mahela *et al.*, 2020b], and islanding detection [Mahela *et al.*, 2020a]. ST and HHT process negative sequence current and voltage signals to obtain islanding and fault detection features in [Swarnkar *et al.*, 2021] within 10ms. Two thresholds are proposed to discriminate between faults, islanding, and other non-islanding transients. An index is proposed by multiplying the features of the S-Transform and Wigner distribution function to detect faults in an IEEE 13 bus system in the presence of noise [Kulshrestha *et al.*, 2020]. A current-based Wigner distribution function and voltage-based alienation coefficient are utilized for proposing a fault index in [Ram Ola *et al.*, 2020]. However, islanding and fault location are not considered in this algorithm.

Transient monitoring function index is proposed by processing the voltage signal at DG location using Fourier-Taylor transformation (FTT) [Dubey *et al.*, 2019]. A threshold of 0.5 is proposed for islanding detection in 55 ms. Kalman filter is utilized to process the voltage signal at DG terminals in [Haider *et al.*, 2018]. First the voltage signals undergo modal tranformation and then KF is applied to obtain the residual signal. The selected harmonic distortion (SHD) is used as an index to detect islanding if it exceeds a threshold of 3. IEEE standard 399 benchmark system is tested with hybrid PV and wind energy sources to achieve the islanding detection within 1-2 cycles. A Gauss-Newton Algorithm for islanding detection is reported in [Padhee *et al.*, 2012].

The time of detection of islanding for various SP techniques with DG used is mentioned in Table 2.3.

D. Fault Detection and classification

Similar to islanding detection, the fault is also detected and classified by comparing the fault-specific features with a threshold. Intermittent earth faults are detected using zero sequence components from current, voltage, and their phase difference. The zero sequence components are processed by Haar wavelet to obtain various high frequency components using which an index is computed, which is compared with a threshold to determine the fault [Lorenc *et al.*, 2003]. A similar algorithm using the phase difference of wavelet coefficients obtained using Morlet-type mother wavelet from the zero sequence voltage and current signals is proposed [Michalik *et al.*,

Table 2.3: Islanding detection time using SP techniques.

SP Technique	Reference	DG used	Detection time	Noise in dB
FT	[Kim, 2012]	Solar PV	1 ms	NC
	[Kim *et al.*, 2011]	Solar PV	<two cycles	NC
WT	[Zhu *et al.*, 2008]	Grid-tied DG	0.6 s	NC
	[Hsieh *et al.*, 2008]	DG at petroleum company	0.05–1 s	NC
	[Pigazo *et al.*, 2008]	Solar PV	0.5–30 cycles	NC
	[Samantaray *et al.*, 2009b]	Wind farm (DFIG)	one cycle	NC
	[Hanif *et al.*, 2010]	Solar PV	2.5 cycles	NC
	[Karegar and Sobhani, 2012]	wind DG	<0.2 s	NC
	[Hanif *et al.*, 2012]	Solar PV	0.05 s	NC
	[Sharma and Singh, 2012]	Solar PV	>one cycle	NC
	[Shariatinasab and Akbari, 2010]	Synchronous DG	5.5 ms	NC
	[Morsi *et al.*, 2010]	Wind farm	0.06 s	NC
	[Samui and Samantaray, 2012]	Hybrid (three wind farms and Gen. set)	10 ms	NC
ST	[Ray *et al.*, 2011]	Hybrid (PV, fuel cell, and wind)	26–28 ms	20
	[Samantaray *et al.*, 2010]	Wind farm	25 ms	NC
HHT	[Niaki and Afsharnia, 2014]	Inverter-based DG	<two cycles	NC
	[Chaitanya and Yadav, 2018]	Synchronous generator	17 ms	40
MM	[Mohanty *et al.*, 2014]	Hybrid (PV and wind)	22 ms	20
	[Farhan and Swarup, 2016]	Hybrid (Diesel and Wind generator)	20 ms	NC

2006]. The algorithm is not affected by the energizing of the feeder or capacitor.

In [Gautam and Brahma, 2012], extracted features from the voltage waveforms from the secondary voltage transformer using mathematical morphology. It is capable of differentiating faults from other events such as changes in loads, capacitor switching, etc. Faults are successfully detected in a distribution system containing rapid earth fault current limiters by [Barik *et al.*, 2017]. Features are obtained from MM by closing opening difference operation (CODO) and are compared with thresholds to determine the presence of a fault and also the faulty phase in the system.

Differential energy based algorithm is proposed in [Kar and Samantaray, 2014b] for fault detection in a microgrid in both grid connected and islanded mode of operation. The current signals measured at both the ends of the feeder are processed by S-transform to obtain energy based features. The difference in the energy is compared with thresholds to determine the various types of faults. The faults can be detected within 4 cycles from the inception of fault without any test case including noise.

Only current signals measured at the substation are processed with ST to obtain the peak magnitude of second harmonic content [Shaik *et al.*, 2019a]. This is used as a fault index to compare with a threshold to detect and classify faults within 40% of a cycle in an IEEE 13 bus system in the presence of Solar PV. The proposed algorithm is not affected by non faulty transients and noise upto 25 dB SNR.

HHT is utilized in [Gururani *et al.*, 2016] to propose a differential scheme for microgrid protection of a 14-bus test system. HHT processes the current signals at both ends of the feeder to obtain IMFs. The suitable IMF is selected by mutual information technique, and the first IMF is considered to obtain the energy content whose difference is used as a feature. The algorithm has a faster detection time when compared to the ST-based differential scheme. The main disadvantage of the differential scheme is the measurement at both ends of the feeder. For multiple feeders, these algorithms require a lot of measuring devices.

In [Li *et al.*, 2021], a differential and summation method using HHT is presented. The instantaneous phase difference of the first IMF is used as a feature to determine various faults. Feature from the zero sequence component is used to compare with a threshold to differentiate LL and LLG faults.

A modified EMD known as complete ensemble empirical mode decomposition with adaptive noise (CEEDMAN) is proposed in [Wang *et al.*, 2018] to decompose the zero sequence current signal to obtain the first IMF. Instantaneous amplitude and instantaneous phase-based features are obtained using HHT to detect and classify the faults using the voting fault detection method.

Teager-Kaiser energy operator (TKEO) based algorithm is proposed in [Jarrahi *et al.*, 2020] for microgrid protection. The sum of the squares of the phase currents is used as signal for processing with a TKEO to obtain an index which is compared with a threshold to detect fault. The fault type is classified by obtaining three similar indices for each phase. The ratio of half cycle data before the fault and after fault is computed as index for each phase. The faulty phase is determined if the proposed index is greater than a prescribed threshold. The involvement of ground is determined by the computation of neutral current and a threshold is proposed for the same. The algorithm is tested on various test systems with variations of fault type, fault location, fault inception angles, fault resistance in the presence of noise upto 20 dB SNR. However, fault location is not considered.

Though some of the algorithms mentioned above perform well in the presence of noise, the incidence angle influence on switching transients is not considered. Also, islanding detection and fault location are not considered.

2.4 MACHINE LEARNING BASED ALGORITHMS FOR ISLANDING AND FAULT CLASSIFICATION

The threshold-based techniques discussed in the previous section requires a thorough study of the system for all the test cases to decide on the threshold value. If the appropriate threshold is not selected, there is a high chance of unnecessary tripping of DG. If a large value is selected, the islanding may not be detected. Also the variations in system configurations leads to adjustment of the threshold setting. This can be is eliminated with the help of machine learning techniques which only requires feature vector input to obtain the desired output without manual threshold selection. These ML techniques generally are associated with signal processing techniques for better feature extraction, resulting in faster detection and less computation.

The authors in [Vatani *et al.*, 2015] used the measurements of voltage, active and reactive powers at DG terminals to obtain the equivalent reactance viewed at the DG. FFT is employed to obtain the harmonic content of the equivalent reactance, and two features are given as input to the DT to classify the islanding. This algorithm is tested on a nine bus system with synchronous DG. The islanding is detected in 300 ms with an accuracy of 100% with DT, 90.9% with ANN and 90.48% with SVM in a noiseless environment. The non islanding cases considered are single phase to ground faults, three phase to ground faults, DG trip, capacitor switching, and load insertion and rejection at DG. FFT is used to extract the harmonic signature of the inverter output voltage, which is used as an islanding detecting feature for Artificial Immune System (AIS) [Yin, 2005].

In [Kar and Samantaray, 2014a], the combination of DFT and data mining algorithms like DT, RF, and SVM are utilized for islanding detection within 1.5 cycles. The voltage and current signal at the target DG location are decomposed to obtain the harmonic information, and 27 features were proposed for islanding detection. The proposed algorithm is tested on an IEC 17-bus microgrid system with synchronous and inverted-based DGs. The non islanding cases considered were DG trip, loss of power on PCC, loss of distribution lines, load variations, and capacitor switching. The faults and noise cases are not considered. The accuracies obtained are 100%, >99%, and >96% for Random Forest (RF), DT, and SVM, respectively.

IDM using multivariate analysis to extract 11 time-domain features is proposed in [Far *et al.*, 2012]. A data mining algorithm is utilized, and a comparison is made with passive methods like under/over voltage, under/over frequency, and ROCOF to prove its superiority. The islanding detection is achieved in 734 ms on an eight-bus system integrated with two synchronous generators. Non islanding cases such as fault, load variations and lines' disconnection are considered in a noiseless environment.

In [Abd-Elkader *et al.*, 2014], second harmonic information from the symmetrical

components of the voltage and current signal is extracted as a potential feature. This feature is fed to a two-layer feed-forward Artificial Neural Network (ANN) to detect the islanding in less than two cycles. The test system considered was a five bus system integrated with wind energy. The algorithm classifies the non islanding cases of a voltage dip, voltage swell, and load switching. The fault and noise cases are not considered.

An algorithm based on the WT of the current and voltage signals at DG locations is reported in [Lidula and Rajapakse, 2010]. The transient energy features are extracted after decomposition using db4 mother wavelet. These features are fed to a DT to classify islanding from other non islanding cases, which include faults, switching transients, and transformer energization. The algorithm is tested on a CIGRE MV benchmark test system having an induction generator and synchronous generator. The islanding classification is performed in 23.9 ms (two cycles) with an overall accuracy of >98%. The same work is extended in the presence of another VSC-based DC source to detect the islanding in 30 ms with an overall accuracy of 96.11% [Lidula and Rajapakse, 2012]. This algorithm works well with a single DG or in a hybrid configuration but the performance decreases with noise less than 50 dB SNR.

In [Shayeghi and Sobhani, 2014] the authors employed Adaptive Neuro Fuzzy Inference System (ANFIS) and DWT for islanding detection. Haar mother wavelet is used as a basis function to decompose the energy signal to extract four features which are fed to ANFIS to classify the islanding within two cycles in a grid-connected inverter-based system. Nonlinear load switching, capacitor switching, various power imbalance conditions, and motor starting are considered in the non-islanding class.

In [Heidari *et al.*, 2013], voltages transient signal is measured to extract the energy features using DWT. These are later fed to a DT to classify the islanding within one cycle. It is reported that the implementation is easy with high accuracy. The accuracy achieved is greater than 98% when tested on a CIGRE MV 30 node network.

A DWT and ANN-based algorithm is proposed in which the voltage signal at the DG side (PV inverter) is decomposed with db1 mother wavelet up to seven levels [Fayyad and Osman, 2010]. The sum of energies of detail coefficients at all frequency levels of all the phases are taken as the feature to feed the ANN. The accuracy obtained was more than 97% at both the DG locations. A comparison with other passive techniques proves that the SP and ML-based method is superior.

In [Mishra *et al.*, 2016b], ST is employed to obtain the time-frequency features from negative sequence current and voltage at DG terminals. Four features based on energy and STD are obtained and trained with various ML techniques like ANN, SVM, and Extreme Learning Machine (ELM). The authors have considered a radial 13 kV feeder of 30 km length integrated with a synchronous generator and an asynchronous hydro generator. The islanding is classified within one cycle from non-islanding events like faults, sudden load change, tripping of DG, switching of the capacitor, and PQ disturbance of voltage sag and swell in noisy conditions. The reported accuracy with all ML techniques was 100% without noise, but ELM obtained good accuracy in the presence of noise, 97.27% at 30 dB and 91.51% at 20 dB when compared to ANN and SVM.

Discrete fast S-transform (DFST) and Fuzzy expert system to achieve islanding and non-islanding classification in [Dash *et al.*, 2012]. The algorithm is tested on a CIGRE North American MV benchmark system integrated with hybrid DGs of synchronous generator, wind farm, solar, and Diesel engine. DFST processes the negative sequence components of current and voltage to obtain S-matrix from which spectral energy contents and standard deviation are obtained as features. A fuzzy expert system is trained with these features to obtain an accuracy of >99% without noise and 97.32% at 20 dB SNR within one cycle. The sampling frequency of 3.84 kHz is considered with non-islanding cases, including faults and variation of configurations from radial to loop.

Table 2.4: Islanding detection time using SP+ML techniques.

SP+ML Technique	Reference	Time of Detection	Accuracy	
			Noiseless	Noisy
FFT+ RT			100%	
FFT+DT	[Kar and Samantaray, 2014a]	<1.5 cycles	>99%	NC
FFT+SVM			>96%	
FFT+ DT			100%	
FFT+ANN	[Vatani *et al.*, 2015]	300 ms	90.9%	NC
FFT+SVM			90.48%	
DWT+DT	[Lidula and Rajapakse, 2010]	23.9 ms (<2 cycles)	99.61%	NC
DWT+DT	[Heidari *et al.*, 2013]	<1 cycle	> 98%	NC
DWT+ANN	[Fayyad and Osman, 2010]	<1 cycle	$\geq$ 97%	NC
DFST+Fuzzy rule	[Dash *et al.*, 2012]	<1 cycle	100% approx	>97% (20 dB)
WT+ANN, WT+SVM ST+ANN,ST+SVM	[Mishra and Rout, 2016b]	<1 cycle	$\geq$ 99%	$\geq$ 90%(20dB)
WPT+ELM	[Mishra *et al.*, 2016c]	<1 cycle	100% approx	$\geq$ 95%(30dB)
ST+DT	[Samantaray *et al.*, 2011]	<2 cycle	100% approx	$\geq$ 96%(20dB)

A WPT and ELM-based islanding classification technique is proposed with a feature index termed change-of-power-index, calculated at different nodes using WPT [Mishra *et al.*, 2016c]. The islanding is classified from non-islanding events with an accuracy greater than 99% without noise and above 95% with the noise of 30 dB.

Features such as STD, energy, kurtosis, and skewness are obtained by analyzing the negative sequence voltage signal through various SP techniques like HST, TTT, and MM methods in [Mohanty *et al.*, 2014]. These features are used to train SVM for classification between islanded and non-islanded events. A comparative study proved that HST, TTT, and MM-based combination with SVM methods perform better than ST and WT-based methods even in the presence of noise.

In [Shayeghi *et al.*, 2016], an ANFIS-based islanding classification algorithm is proposed and tested on an IEEE 34 bus system with five DGs. The input signals are optimally selected by decomposing them at various levels and using various mother wavelets using WT. The standard deviation of the energy of the signals is selected as a criterion for selecting the inputs. Later these selected features are used to train ANFIS using various training algorithms like Particle Swarm Optimization (PSO), Genetic Algorithm (GA), Ant colony, and differential evolutional algorithm for obtaining better accuracy. However, the algorithm fails to classify non-islanding events, including various switching transients for noise levels below 45 dB. Faults are not simulated in this study. The Table 2.4, enumerates the different SP + ML techniques for islanding classification and the time of detection with accuracies.

Various methods are proposed for fault detection and classification in the literature using SP and ML techniques. The first three IMFs were obtained from the voltage signal by EMD in [Manjula *et al.*, 2011]. Later energy and SD of instantaneous features of amplitude and phase are given as training inputs of Probabilistic Neural Network (PNN). The faults are classified into four classes of LG, LL, LLG, and LLL to obtain an accuracy of 94.06% and 90.93% with WT and PNN.

Similarly the fastest fault detection times using the combination of SP and ML techniques is obtained using a combination of DWT and SVM in 0.5 cycles [Deng *et al.*, 2015], combination of ST and PNN in 0.5 cycles [Samantaray *et al.*, 2008], fuzzy based technique in 0.5 cycles [Das, 2005], Wavelet and Data mining technique within 1 cycle [Mishra *et al.*, 2015], fast discrete S-Transform and Extreme Machine learning in 1 cycle [Mishra and Rout, 2019], Hilbert Huang Transform and Extreme learning machine in 6 cycles [Mishra and Rout, 2018]. However, in all the above methods, the distribution system was different, and also only fault detection was considered without islanding detection and or noise presence in many cases. Therefore a comparison is made on the methods proposed for the protection of the standard radial IEEE 13 bus system. The table gives the different methods and accuracies obtained on an IEEE 13 bus system. In the methods discussed in Table 2.5,

Table 2.5: Comparison of recent work on IEEE 13 bus system.

Reference	Method	Accuracy			Number of Classes	Measurements	Fault location
		No Noise	30 dB	20 dB			
[Mishra and Rout, 2019]	FDST+ RELM	100	98.78	90.00	2 classes	V and I	NA
	FDST+ BELM	100	98.78	91.5			
[Shafiullah *et al.*, 2018]	ST+FFNN	99.47	99.14	99.02	2 classes	Only I	NA
[Mishra *et al.*, 2017]	HHT-ANN	93.63	88.45	83.33	2 classes	Only V	NA
	HHT-SVM	96.36	90.93	85.45			
	HHT-RELM	97.57	91.01	90.00			
	HHT-BELM	98.5	95.95	90.04			
	HHT-WBELM	99.09	98.08	96.06			
[Alshareef *et al.*, 2014]	WT+Ensemble Tree Classifier	>95	NA	NA	2 classes	Only V	NA
	WT+SVM	>99					

the classification is predominantly a two-class problem fault/no fault or islanding/non-islanding. FDST and ELM combination is used in [Mishra and Rout, 2019], in which the islanding and non-islanding classification is done within one cycle. The faults, power quality disturbances, and switching transients are clubbed into the non-islanding class. Here both the voltage and current signals are measured.

In [Shafiullah and Abido, 2018], the combination of ST and Feedforward Neural network (FFNN) is utilized to classify two classes of the fault and no fault. Only load variation is considered in nonfaulty cases without an islanding case study. The features after HHT are fed to various ML algorithms like ANN, SVM, and ELM in [Mishra *et al.*, 2017]. Here also, the classification is done as a two-class problem of islanding and non-islanding. In the non-islanding case, all the faults and nonfaulty transients and switching transients are considered to achieve the classification within one cycle. Similar work is done in Alshareef *et al.* [2014], in which a new WT (WGM1.0) with ensemble tree classifier (ETC) and SVM are proposed. However, the effect of noise is not considered in this work. Therefore a faster detection of 1 cycle is achieved. It can be observed that the fault detection and switching transients are not considered separate classes, and also, the fault location is not accomplished. Though fault incidence angles are considered, the effect of incidence angle on switching transients is not considered in any study. In all the methods, the accuracy of classification decreased with an increase in noise. The best accuracy obtained is using HHT as a preprocessor in [Mishra *et al.*, 2017] with 96.06% at 20 dB SNR.

2.5 FAULT LOCATION METHODS

In addition to fault detection and classification, fault location in distribution system is challenging due to shorter distribution lines, complex laterals, unbalanced operation and time varying load profile [Gururajapathy *et al.*, 2017]. The fault location methods can be categorized as impedance based methods, travelling wave based method, algorithms based on sparse measurements, signal processing and ML methods [Bahmanyar *et al.*, 2017]. These techniques are reviewed as following.

2.5.1 Impedance Based Method

The fault location using the impedance-based method utilizes the information at the substation, such as fundamental frequency, voltage, current measurements, line data, load data,

and network topology. Since the distribution feeders also have intermediate loads, the distance to the fault from the measuring point or substation is estimated by considering the first line section and iteratively solving the equations describing the steady-state fault conditions for all the line sections one after the other. The fault analysis is done using symmetrical components or in phase domain. The algorithms proposed in [Girgis *et al.*, 1993], [Das *et al.*, 2000], [Yang *et al.*, 2008], [Das *et al.*, 2012] and [Dashti and Sadeh, 2014] utilized symmetrical components.

The faulted circuit analysis in phase domain is researched in [Zhu *et al.*, 1997], [Choi *et al.*, 2007], [Filomena *et al.*, 2009], [Salim *et al.*, 2011].

An estimated fault location ds in case of an AG fault in a line section is proposed in [Lee *et al.*, 2004], obtained as equation (2.19), with upstream current phasors $Is = [Ia, Ib, Ic]^T$ and the sending end voltage $Vs = [Va, Vb, Vc]^T$:

$$ds = \frac{V_a^{re}(I_a^{im} - I_L^{im}) - V_a^{im}(I_a^{re} - I_L^{re})}{A(I_a^{im} - I_L^{im}) - B(I_a^{re} - I_L^{re})} \tag{2.19}$$

where, re, im indicate the real and imaginary parts of phase-A, I_L = load current during the fault, Zl =line impedance matrix, and A and B are defined as:

$$A = {Zl_{aa}}^{re} I_a^{re} - {Zl_{aa}}^{im} I_a^{im} + {Zl_{ab}}^{re} I_b^{re} - {Zl_{ab}}^{im} I_b^{im} + {Zl_{ac}}^{re} I_c^{re} - {Zl_{ac}}^{im} I_c^{im} \tag{2.20}$$

$$B = {Zl_{aa}}^{re} I_a^{im} + {Zl_{aa}}^{im} I_a^{re} + {Zl_{ab}}^{re} I_b^{im} + {Zl_{ab}}^{im} I_b^{re} + {Zl_{ac}}^{re} I_c^{im} + {Zl_{ac}}^{im} I_c^{re} \tag{2.21}$$

The unknown values of I_L and ds are computed iteratively by solving the equations with an initial guess of the values. If the estimated fault distance converges to a distance less than the line section length, then the fault location is confirmed in that section. Otherwise, the following line section is considered, and the process is repeated for all the line sections with the voltage and current values of the section heads till the estimated fault location is less than the length of the line section. The equations for other types of faults can be obtained similarly and solved in the impedance-based methods.

In the case of many laterals in the distribution feeder, the equivalent impedance method is proposed in [Choi *et al.*, 2007], representing line and loads as constant impedances. For heavily branched distribution networks, the method proposed in [Salim *et al.*, 2011] uses algorithms to perform power flow with pre-fault substation currents and voltage, and the equivalent impedance Z_{m-n} is calculated in each node applying equation (2.20):

$$Z_{m-n} = \frac{V_m}{I_{m-n}} \tag{2.22}$$

where, V_m and I_{m-n} are pre-fault voltage at node m and the pre-fault current flowing from node m to node n respectively.

The factors affecting impedance-based methods' performance include load and line modeling. Customer loads are simulated either as constant impedance load models or voltage-dependent load models. The load current uncertainties do not affect the fault location estimation unless the fault resistance is too high. Depending on the line length, the models should incorporate shunt capacitance if they are not short. Long overhead and underground cables give accurate fault distance estimates if modeled in detail [Yang *et al.*, 2008]. However, the computational burden also increases. Hence a trade-off is made between accuracy and the computational requirement for proper choice of the line and load modeling [Mora-Florez *et al.*, 2008].

One of the disadvantages of these methods is the multiple estimations of the fault location, as the impedance can be seen as the same for various possible fault locations from the measuring point.

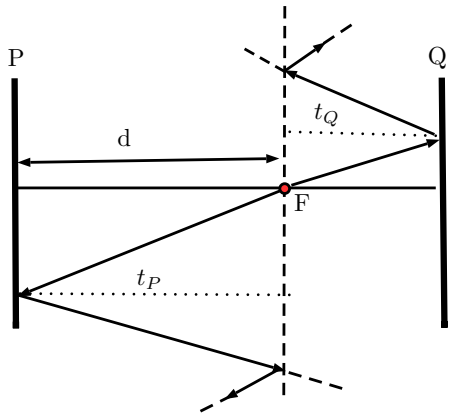

Figure 2.4: Travelling wave lattice diagram

Some solutions are proposed to solve this issue by utilizing the information of the current patterns and the protective devices in the faulted path [Lee *et al.*, 2004]. The installation of fault indicators, which requires a communication network and is costly to implement, is proposed in [De Almeida *et al.*, 2011]. Load current information of nonfaulty phases is utilized in [Krishnathevar and Ngu, 2011]. Integration of two fault location methods is proposed in [Lotfifard *et al.*, 2012]. The voltages measured at the DG terminals are also utilized to overcome this issue [Alwash *et al.*, 2014]. Smart meters are also promising candidates to solve the multiple location problems in modern distribution systems.

2.5.2 Travelling Wave Based method

Traveling wave based method is based on the concept of traveling and reflected waves between the line terminals and the fault location in the network until a post-fault steady state is reached [Van der Sluis, 2001]. The traveling waves emanate from the fault or the discontinuity in the line and travel towards both terminals. These get reflected at the terminals towards the fault. At the fault point, the incident traveling wave is reflected as one part towards the terminal while the other travels beyond the fault. Faults can be located by measuring the travel time of these waves at both the terminals. These methods are widely applied for transmission line fault locations and are now utilized in distribution systems. They are accurate and fast but require advanced measurement and communication infrastructure like GPS.

Let t_P = travel time from the fault to the line terminal P and t_Q = travel time from the fault to the line terminal Q as shown in Fig. 2.4, the delay in detection times at the two terminals is obtained by equation (2.23) and the fault distance is obtained by equation (2.24).

$$t_d = t_P - t_Q \tag{2.23}$$

$$d = \frac{L_l - v t_d}{2} \tag{2.24}$$

where, L_l is the line length, v is the velocity of the traveling waves, and d is the distance between line terminal P and fault.

Traveling wave methods depend on signal processing techniques like wavelet transform to extract the transients or characteristic frequencies corresponding to the fault locations. In [Nouri *et al.*, 2001], a method is proposed for the distribution network inspired by the standard two-end fault location method [Magnago and Abur, 1998] for the transmission lines. Discrete wavelet

transform (DWT) is used here to obtain transient information at the substation and all the load terminals, though not practical to measure at each terminal at the distribution level. A single-ended fault location method with a high pass filter is used in [Thomas *et al.*, 2003] to extract the fault transients.

More methods are proposed as the standard techniques of transmission lines are not applicable for distribution systems due to complex network topology and several reflections. In [Bo *et al.*, 1999], the high-frequency information of voltage signals extracted using a band-pass filter is utilized. Their arrival is identified successively at one locator. The time delay between the first and the next transient signals is used to identify the fault position. Similarly, in [Hizman *et al.*, 2002], high-frequency current transients are first utilized for locating the faulty section. Subsequently, faults are simulated along this section to cross-correlate with the recorded waveforms to locate the fault. In [Sadeh *et al.*, 2013], the authors proposed a modal transformation of the voltage signal fault transients from the phase domain. A comparison with an offline database containing simulated data is utilized for fault location.

In [Borghetti *et al.*, 2006], CWT is applied on voltage signals to obtain fault transients. These transients are matched with the calculated frequencies at different fault locations to ascertain the fault location. This method is improved and proven better for different laterals and tappings of load by identifying a specific mother wavelet from the recorded voltage transients after faults [Borghetti *et al.*, 2008]. A time-stamping method is proposed to locate faults even on branches [Robson *et al.*, 2014]. In [Goudarzi *et al.*, 2015], CWT and DWT are integrated to minimize the requirement of fault recorders.

One of these methods' limitations is the requirement of a higher sampling frequency of measuring devices as high as 1 MHz [Goudarzi *et al.*, 2015] to 10 MHz [Borghetti *et al.*, 2010]. Despite advancements in transducer technology to achieve such higher sampling rates, it becomes expensive at the distribution level. Unlike the impedance-based methods, the traveling wave-based fault methods are least affected by modeling errors, but laterals and load tappings in the distribution network affect their performance. Impedance-based methods and traveling wave-based techniques, which are traditionally used, do not provide exact fault location if the distribution system is extensive and heavily branched. A combination of these methods is proposed in [Gazzana *et al.*, 2014] to avoid multiple estimates of the fault location.

2.5.3 Sparse Measurements Method

These methods utilize the measurements from sparse meters like digital fault recorders, power quality meters, etc., installed all over the distribution network. They require good communication infrastructure. Whenever there is a fault in the network, voltage sags occur at different nodes with varying characteristics. The concept is to measure these voltage sags at specific nodes to find the possible fault location. Therefore these are also called voltage sag-based methods. Since the prior knowledge of fault is unknown, estimating the current and resistance is required.

An algorithm is proposed by creating a database of voltage sags for faults at various sections [Mokhlis and Li, 2007]. The faulty section is identified when a fault occurs by comparing the recorded voltage sag with the database. This method was extended and improvised results are reported in [Mokhlis *et al.*, 2010].

In [Brahma, 2011], an algorithm is proposed in which the estimated fault current and three-phase bus impedance matrix are utilized to compute the voltage variations at each node. The fault current, though estimated as the sum of the fault currents from all the sources, causes errors. The faulty node is then identified by comparing the calculated and measured voltages. A similar method is proposed in [Trindade *et al.*, 2013], in which the fault current is compared at each node using the measured voltage and three-phase bus impedance matrix. One limitation is that

this method requires a large number of meters for better results.

An error index is proposed in [Pereira *et al.*, 2009], and the fault node with with minimum error is designated as the fault location. It also requires less number of voltage measurements. Similar error index is proposed in [Dong *et al.*, 2013] applicable only to single-line to ground faults.

A state estimation-based algorithm is proposed to improve the overall accuracy, but it demands a computational burden [Jamali and Bahmanyar, 2016]. The authors in [Majidi *et al.*, 2014a] proposed a compressive sensing technique with the help of phasor measurement units (PMU) for fault location in distribution networks which work well in the presence of noise. The same algorithm is improvised with the help of the k-nearest neighborhood for locating all types of faults and the Fuzzy c-mean method to locate simultaneous faults [Majidi *et al.*, 2014b]. These methods avoid the multiple estimation problem associated with impedance-based methods. However, they require the installation of measurement devices along the distribution feeder.

2.5.4 Signal Processing and Machine Learning Methods

The previously discussed methods are based on mathematical computations after the fault. The suitability of fault location methods also depends on the neutral point's effective grounding. Machine learning techniques are efficient even when the system conditions are unpredictable such as in distribution networks. The output is generally the fault distance, and the inputs comprise features from voltages or currents. It requires extensive training data from simulated or real scenarios to establish a complex relationship between input and output.

A back-propagation NN is used to detect and locate high impedance faults (HIF) in distribution systems in the presence of DG with current, and voltage signals given as input Bretas *et al.* [2006]. A multilayer perceptron (MLP) neural network is proposed in Javadian *et al.* [2009] to identify fault types and locations in a simulated 16 bus, 20 kV distribution network in the presence of a diesel generator. The ratio of the injected fault currents of DGs to the substation current is selected as input to minimize fault impedance's effect. A separate MLP is proposed to estimate the fault distance from DGs and substation depending on the fault type. In order to improve the convergence rate Levenberg-Marquardt algorithm is used for training the neural network. A Radial Basis Function Neural Network with Optimum Steepest Descent (RBFNN–OSD) learning algorithm is proposed in [Zayandehroodi *et al.*, 2013]. Two Neural Networks are developed for various types of faults. One NN estimates the distance from the source and DG units, and the other identifies the exact faulty line.

The authors in Aslan [2012] proposed a fault classification and location algorithm by training the voltage and current samples from the source to an FFNN to obtain the fault distance from the source. A 34.5 kV distribution feeder of 40 km with load taps at every 10 km is simulated in EMTP. A maximum percentage error of 3.16% and 4.86% are reported for faults at 12.5 km and 25 km from the source, respectively, using one cycle post-fault data. The same method was implemented on an actual distribution feeder located in Turkey by considering the fault resistance, fault angle, and source capacity effects in Aslan and Yağan [2017].

In Dehghani and Nezami [2013] fault distance is estimated in an IEEE 34 bus system without DG by giving the measured current, voltage, and active power of the feeder at the substation as input to ANN. The three-phase current signals and zero sequence current are decomposed using discrete wavelet transform up to five levels, and features such as energy entropy per unit are given as input to ANN to locate the fault in IEEE 34 bus system Adewole *et al.* [2016]. The fault location nearest to the source is considered as 34.96 km, reporting an error of 1.54%.

In [Rafinia and Moshtagh, 2014], a fault classification and location algorithm is proposed for a 20 kV underground distribution network. Wavelet transform is applied on both voltage and

current signals to obtain eighth-level details using the db4 mother wavelet. Statistical features are then computed as input to a three-layer feed-forward ANN and a fuzzy logic system to classify the type of fault and estimate the fault location. A similar approach is followed in [Nikhli and Safavi, 2011] to extract energy features after decomposition of voltage signal using wavelet transform and train a FFNN.

A combination of WT and ANFIS is proposed in [Mora *et al.*, 2006]. A novel wavelet fuzzy neural network (WFNN) is proposed in [Chunju *et al.*, 2007]. A combination of HHT and ANN is utilized in Kang *et al.* [2013]. In this algorithm, the extracted energy features of zero sequence current from the Hilbert Huang transform are given as input to locate the fault. ANN-based fault location algorithm using regularized radial basis function (RRBF) on a 13 bus distribution system is proposed in [Tong *et al.*, 2018]. The current, voltage amplitude and angle are utilized to find the faulty zone, followed by the exact fault location. Phasor Measurement Unit (PMU) devices are employed in each busbar to obtain the required data.

The authors in [Thukaram *et al.*, 2005] considered a practical 52 bus distribution system for their study. Initially, SVM is used to classify the faults into four classes. Later ANN is utilized to estimate the fault reactance from the measuring point. Three-phase steady-state voltage and current measurements analyzed with PCA are given as inputs. An SVR-based fault location estimation algorithm is proposed for a four-bus system using the features from DWT [Ye *et al.*, 2014]. It is reported that the SVR performed better than ANN for a few training samples. A fault location method based on SVM for a non-effectively grounded two-bus ring system was proposed by [Deng *et al.*, 2015]. Firstly the faulty section is identified by the variation of zero sequence current before and after closing the switch in the loop network. Secondly, the zero sequence current is decomposed using wavelet transform to extract eigenvalues and given as input to train SVM and estimate the fault distance.

A combination of wavelet and ELM is proposed in [Shafiullah *et al.*, 2017] for fault location in IEEE 34 bus system. The performance is compared with other ML techniques, and reported ELM performs better than SVR and ANN. Similar work is done using features extracted from ST and fed to an ELM to find the fault location in IEEE 13 bus system Shafiullah *et al.* [2018]. However, the method requires measurements from eight different locations. Genetic algorithm-based fault location techniques are also reported in [Jamali *et al.*, 2015],Jin and Ju [2012].

The features based on EMD of transient voltage signal are utilized for fault location in IEEE 34 bus system. The energy content of the intrinsic mode functions is fed as input to the core vector regression (CVR) model for locating faults in the distribution system in [Khorramdel *et al.*, 2014]. A comparison is also made with ANN-based fault locator, but they do not perform well for faults closer to measuring bus. The fault at 0.6 km has a location error of 315m or 52.5%. Also, the ANN-based method shown in the same paper has an estimated error of 550m or 91.67%.

The tree-like logic flow is also employed for power system fault diagnosis based on the extracted features from faulty signals. Comparisons are made at each stage of the logic flow with pre-fixed thresholds to arrive at a decision. A tree-structured fault location algorithm is proposed using thresholds to locate faulty zone in an IEEE 13 bus system [Shaik *et al.*, 2019c]. However, 100% data was used for fixing thresholds, and the probability of failure stands high with new data in the presence of noise. Hence, DT based learning approach is most suitable.

In Zhao *et al.* [2019] an algorithm is proposed based on a random forest algorithm. The short circuit fault currents obtained from feeder terminal units (FTUs) are used as features to achieve both single and multiple fault section locations in distribution networks. An algorithm is proposed in Okumus and Nuroglu [2021], in which the WT is used to extract detail coefficients from voltage and current signals at various levels using Daubechies mother wavelet. Features are computed using these detail coefficients and given as input to a random forest to obtain the faulty section in an IEEE 34 bus system.

Decision tree regression (DTR), a robust data mining tool, was employed for fault location in an IEEE 14 bus system using features from discrete wavelet transform (DWT) and discrete Fourier transform (DFT) in [Swetapadma and Yadav, 2016]. The maximum errors reported were 400m and 200m for faults at 600m and 800m from the measuring point, respectively. In order to have an automated distribution system, the faults closer to the measuring bus have to be estimated correctly.

Another desirable aspect from the fault location algorithms is to minimize the measuring quantities by the usage of only features from current signals [Abdullah, 2017].

2.6 RESEARCH GAPS IDENTIFIED

Though a lot of research is reported in this field using signal processing and machine learning algorithms there is always a room for improvement by researching efficient features to minimize the detection time. The gaps identified from the research are listed here.

- Empirical mode decomposition being an adaptive technique, can be researched further to obtain residue-based features which can potentially remove the selection of IMFs through separate methods like Kurtosis, Mutual Information, etc.
- Fault location in a distribution system having short distribution lines is a big challenge with fair level accuracy for faults near the substation.
- An image-based visually distinct feature for fault detection is rarely reported.
- The algorithms proposed in the literature predominantly used both voltage and current measurement at various measuring points. Hence, there is a need to reduce the parameters to be measured to reduce the cost and complexity of the protection system.
- A fast and complete algorithm to perform islanding detection, fault detection, classification, and location in the presence of noise is a vital need for secure, economic, and reliable performance of utility grid with RE penetration.

2.7 CONCLUSION

This chapter discusses signal processing techniques with their merits and demerits. The various protection algorithms are discussed for islanding, fault detection and classification, and fault location. The detection times and the accuracies obtained with various ML algorithms are presented with a focus on the test system used for the study. The research gaps are identified in the already well-researched field of islanding and fault detection in the presence of renewable energy sources.